

A second-order continuous sliding mode based on DPC for wind-turbine-driven DFIG

Abdelkader Bouyekni, Rachid Taleb, Zinelaabidine Boudjema, Housseyn Kahal

*Electrical Engineering Department, Hassiba Benbouali University, Chlef, Algeria
Laboratoire Génie Electrique et Energies Renouvelables (LGEER)
E-mail: aek.bouyekni81@gmail.com*

Abstract. The paper presents a novel robust direct power control scheme for controlling the stator active and reactive power for a grid-connected doubly-fed induction generator (DFIG) using a second order continuous sliding mode (SOCSM) and a space-vector modulation (SVM). Conventional direct-power control (C-DPC) with hysteresis controllers has significant active and reactive ripples at a steady-state operation and also the switching frequency varies a wide range. The proposed DPC technique based on a second order continuous sliding-mode control reduces the current and torque ripples. Besides, the proposed control scheme is simple to implementation as it does not require the current control loops and transformation coordination's. Simulation results of the proposed controller (SOCSM) and (C-DPC) scheme are compared for various step changes in the active/reactive power. The impact of the machine-parameter variations on the system performance is investigated. Simulation results show the effectiveness of the proposed direct torque control strategy comparatively to the C-DPC one.

Keywords: wind energy; doubly fed-induction generator (DFIG); direct-power control; second-order continuous sliding mode.

Neposreden nadzor moči z uporabo stalnega drsnega načina drugega reda pri dvojno napajanjem asinhronskem generatorju v vetrnih elektrarnah

V članku smo predstavili novo, neposredno močnostno krmilno shemo za regulacijo delovne in jalove moči pri dvojno napajanjem asinhronskem generatorju pri stalnem drsnem načinu drugega reda in uporabo prostorsko-vektorske modulacije. Konvencionalen neposreden nadzor moči s histereznno regulacijo ima znatna nihanja v stacionarnem delovanju in spremembe frekvence v širokem področju. Predlagana metoda na osnovi stalnega drsnega načina drugega reda zmanjšuje spremembe pri toku in navoru. Predlagana metoda je preprosta za izvedbo, saj ne zahteva tokovnih krmilnih zank in transformacij koordinat. Primerjali smo rezultate simulacij pri različnih korakih delovne in jalove moči. Analizirali smo vpliv sprememb parametrov generatorja na zmogljivost sistema. Rezultati simulacij potrjujejo učinkovitost predlagane metode.

1 INTRODUCTION

Wind energy is one of the clean and renewable sources of energy existing in the world. Generally, it has a little direct effect on the environment, as there are no greenhouse-gas or heat emissions or other pollutants. In the last years, a doubly-fed induction generator (DFIG) is most used in the wind-turbine system (WTS) applications [1].

The major advantage of some DFIG is that the power converter has to carry around 30 % of the total power,

so the means size and cost of the converter will be less [2].

Types of the control-strategy behavior of the DFIG-based WTS have been studied [3]. Currently, the conventional scheme control of DFIG through the vector stator-flux-oriented or stator-voltage-oriented vector control is most widely adopted [4, 5]. In this control scheme, decoupling between the d-axis and q-axis current is achieved with a feed-forward compensation, making the DFIG model simples and enabling the use of the PI controllers. Nevertheless, this control structure strongly depends on machine parameters. It uses multiple loops and requires much control-effort to guarantee the structure stability over the total velocity range [6].

To solve the problems of the vector control, DPC control algorithms of DFIGs are discussed in [7, 8]. The C-DPC method can directly control the stator active and reactive powers by using a lookup- Table and hysteresis controllers. However, it has some disadvantages, such as high active-and reactive-power ripples and a variable switching frequency. Using the SVM scheme [9] is interesting for many researchers for its reducing these undesirable effects. Nevertheless, the robustness is low due to the linear control [10- 11].

Some solutions to the problem of the rotor losses with the sliding-mode direct-power control technique used in the induction generator are proposed in [12,13]. In [14],

the researchers use a DPC technique with a second-order sliding mode (SOSM) for controlling the induction generator.

A recent trend, the SOSMs control scheme encompasses all the properties of SMC that affect the second-order time derivatives of the structure system and attenuate the chattering phenomenon, thus reducing mechanical stresses in the system.

This paper presents the fundamental aspects of SOCSM-DPC and pertinent simulation results for a DFIG drive. The proposed strategy is compared with C-DPC. Our original contribution to solving the problem is application of the proposed strategy to control the active and reactive power of DFIG drives supplied by a pulse-width modulation (PWM) inverter. The simulation results prove that SOCSM-DPC has a very robust behavior, like a conventional SMC, and it works with no steady-state chattering. This represents a novel robust and ripple-free DPC method for the DFIG drives control.

2 MODEL OF DFIG

A schematic diagram of the DFIG-based wind-energy generation model is shown in Figure 1 [15].

The model consists of a wind turbine, gearbox and DFIG. Self-commutated IGBT-based two bi-directional voltage-source converters sharing a common dc link are connected between the rotor and stator windings of the DFIG, while the stator winding is directly connected to grid.

A model of the DFIG is presented in literature [16, 17] (Figure 1). In the Park reference frame, the stator and rotor voltage equations of the generator are given as follows:

$$\begin{cases} V_{ds} = R_s I_{ds} + \frac{d}{dt} \psi_{ds} - \omega_s \psi_{qs} \\ V_{qs} = R_s I_{qs} + \frac{d}{dt} \psi_{qs} + \omega_s \psi_{ds} \\ V_{dr} = R_r I_{dr} + \frac{d}{dt} \psi_{dr} - \omega_r \psi_{qr} \\ V_{qr} = R_r I_{qr} + \frac{d}{dt} \psi_{qr} + \omega_r \psi_{dr} \end{cases} \quad (1)$$

Where;

$-V_{ds}, V_{qs}, I_{ds}, I_{qs}, \psi_{ds}$ and ψ_{qs} are the voltages, currents and fluxes, respectively, in a two-phase rotor circuit.

$-V_{dr}, V_{qr}, I_{dr}, I_{qr}, \psi_{dr}$ and ψ_{qr} are the voltages, currents and fluxes, respectively, in a two-phase rotor circuit.

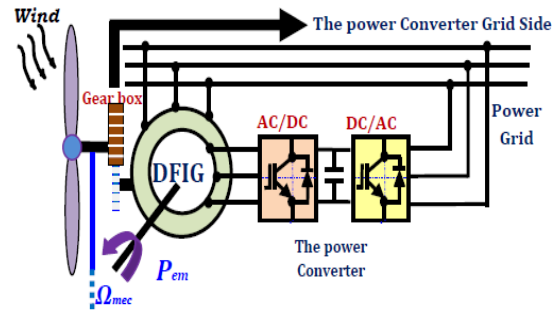


Figure 1. Configuration of the wind energy conversion system based on DFIG.

$$\begin{cases} \psi_{ds} = L_s I_{ds} + M I_{dr} \\ \psi_{qs} = L_s I_{qs} + M I_{qr} \\ \psi_{dr} = L_r I_{dr} + M I_{ds} \\ \psi_{qr} = L_r I_{qr} + M I_{qs} \end{cases} \quad (2)$$

Where L_s , L_r and M are the stator, rotor and mutual inductances, respectively. Then $L_s = L_{ls} + M$ and $L_r = L_{lr} + M$, L_{ls} and L_{lr} are the leakage inductances of the stator and rotor; ω_s , ω_r are the electrical stator and rotor angular speed, according to $\omega_{sl} = \omega_s - \omega_r$, the slip angular speed of DFIG.

The electromagnetic torque in the mechanical equation of DFIG is defined as follows:

$$C_{em} = C_r + J \cdot \frac{d\Omega}{dt} + f \cdot \Omega \quad (3)$$

C_r is the load torque, Ω is the mechanical rotor speed, J is the inertia, f is the viscous-friction coefficient and p is the number of pole pairs.

The electromagnetic torque C_{em} can be expressed as:

$$C_{em} = \frac{3}{2} p \frac{M}{L_s} (\psi_{qs} I_{dr} - \psi_{ds} I_{qr}) \quad (4)$$

According to the active-and reactive-power theory, which is useful in controlling of the power DFIG systems stator-side power components P_s , Q_s can be estimated as:

$$\begin{cases} P_s = \frac{3}{2} (V_{ds} I_{ds} + V_{qs} I_{qs}) \\ Q_s = \frac{3}{2} (V_{qs} I_{ds} - V_{ds} I_{qs}) \end{cases} \quad (5)$$

In this part, we use a synchronous reference frame of the stator active and reactive power by following the state formula when axis d is aligned with the stator-flux vector (Figure 2) [18].

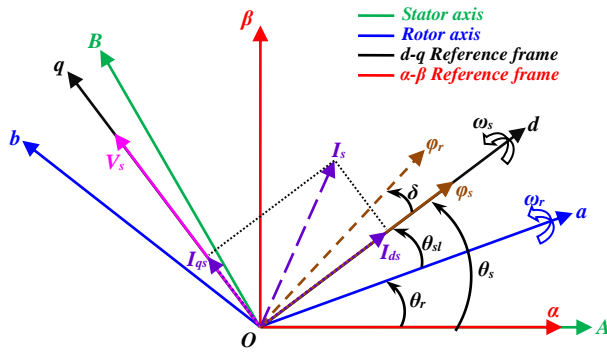


Figure 2. Field-oriented control technique.

By considering the stator resistance, R_s is ignored, hence, we can write.

$$\Psi_{ds} = \Psi_s \quad \text{and} \quad \Psi_{qs} = 0 \quad (6)$$

$$\begin{cases} V_{ds} = 0 \\ V_{qs} = \omega_s \Psi_s \end{cases} \quad (7)$$

$$\begin{cases} I_{ds} = -\frac{M}{L_s} I_{dr} + \frac{\Psi_s}{L_s} \\ I_{qs} = -\frac{M}{L_s} I_{qr} \end{cases} \quad (8)$$

Based on (6), (7), and (8), the instantaneous powers of the stator can be given as:

$$\begin{cases} P_s = -\frac{3}{2} \frac{\omega_s \Psi_s M}{L_s} I_{qr} \\ Q_s = -\frac{3}{2} \left(\frac{\omega_s \Psi_s M}{L_s} I_{dr} - \frac{\omega_s \Psi_s^2}{L_s} \right) \end{cases} \quad (9)$$

The electromagnetic torque can then be expressed by:

$$C_{em} = -\frac{3}{2} p \frac{M}{L_s} I_{qr} \Psi_{ds} \quad (10)$$

3 DIRECT-POWER CONTROL OF DFIG

Using the conventional sliding mode control SMC provides many advantages, such as high robustness and easy implementation. Nevertheless, in this control strategy, the first time derivative directly affects modes the sliding manifold discontinuous.

The major problem of the classical sliding-mode control is the chattering phenomenon caused by the control switching, which may have undesirable effects on the machine, such as overheating of the windings, torque pulsation, current harmonics, acoustic noise, etc. [19].

Many researchers have taken an effort to avoid these drawbacks. The basic idea is to stabilize the dynamics in the small interval in a discontinuous surface without changing the essential characteristics of the whole system. A higher-order sliding-mode HOSM is one of the most efficient methods to overcome these problems. This approach generalizes the essential mode idea that acts on the higher-order time derivatives of the sliding manifold, instead of acting on the first deviation derivative as it happens in conventional (first order) sliding modes [20]. The major properties of the ordinary technique and high control accuracy are presented in [10, 11]. In this way, the chattering phenomenon can be totally attenuated in theory.

The handicap of the HOSM-algorithm implementations is the need of much information, for example the knowledge of $s, \dot{s}, \dots, s^{(n-1)}$ is required to an n -th-order controller.

Among all the algorithms proposed for HOSM, the super twisting algorithm is an exception; it requires only information about the sliding surface [19]. Consequently, this algorithm is used for the proposed control strategy. As in [20], with this algorithm, the stability can be justified for all SOSM controllers.

Using a second-order continuous sliding-mode control is well suitable because of its characteristics, such as robustness under uncertainties. It can also decrease chattering and provides better transient features than some other high-order sliding mode [21].

The proposed control law applied in this paper can be expressed as [22]:

$$u(t) = -l_1 |s|^{a_1} \text{sgn}(s) \dots - l_n |s^{(n-1)}|^{a_n} \text{sgn}(s^{(n-1)}) - v \quad (11)$$

where v is defined by (11)-(12) and scalars a_1, a_2, \dots, a_n satisfy (13). In addition, l_1, l_2, \dots, l_n are the scalar coefficients defined such that the n^{th} -order polynomial $p^n + l_n p^{n-1} + \dots + l_2 p + l_1$ is Hurwitz.

$$v(t) = k \cdot |s|^{1/2} \text{sgn}(s) + v_1(t) \quad (12)$$

$$\dot{v}_1(t) = \alpha \cdot \text{sgn}(s) \quad (13)$$

$$a_{i-1} = \frac{a_i a_{i-1}}{2a_{i+1} - a_i}, \quad i = 2, \dots, n \quad (14)$$

with $a_{n+1} = 1$ and $a_n = a$.

3.1. SOCSM-DPC of the DFIG

SOCSM-DPC consists of describing the method in which the controls of the active and reactive power of DFIG are directly controlled without an intermediate step of using current controllers as in the field-oriented control. In C-DPC, the stator active power is controlled by direct axis voltage V_{dr} , while the reactive power is

controlled by the quadrature axis voltage V_{qr} .

The proposed SOCSM-DPC strategy designed to control the active and reactive power of the DFIG system is illustrated in Figure 3.

The second-order continuous sliding mode active-and reactive-power controllers are designed to change the d and q-axis voltages (V_{dr}^* and V_{qr}^*), respectively, as in (15) and (16).

$$V_{dr}^* = -l_1 |S_{ps}|^{a_1} \text{sign}(S_{ps}) - k_1 \cdot \text{sign}|S_{ps}|^{1/2} + \int \alpha \cdot \text{sign}(S_{ps}) \quad (15)$$

$$V_{qr}^* = -l_1 |S_{qs}|^{a_1} \text{sign}(S_{qs}) - k_2 \cdot \text{sign}|S_{qs}|^{1/2} + \int \alpha \cdot \text{sign}(S_{qs}) \quad (16)$$

Where stator active-power error $S_{ps} = P_s^* - P_s$ and stator reactive-power error $S_{qs} = Q_s^* - Q_s$ are the sliding variables, and constant gains k_1 and k_2 verify the stability conditions.

3.2. Stability and gain choice of SOCSM-DPC

A dynamic system with input u , position x and output y may be given as follows.

$$\frac{dx}{dt} = a(x,t) + b(x,t)u, \quad y = c(x,t) \quad (17)$$

The main problem of the control is to determine input function $u = f(y, \dot{y})$ whereas it can drive the system trajectories to the initial point $y = \dot{y} = 0$ of the phase plane in a limited time. Frame input u is defined as a new state variable and the switching control is applied to its time derivative \dot{u} . Output y is controlled by an SOCSM controller with sliding variable $S = y^* - y$.

This type of the control does not use the derivative of the sliding variable. As in by (15) and (16), the adequate condition for convergence to the sliding surface and for stability that the gains are large enough [14].

$$k_1 > \frac{A_M}{B_m}, \quad k_2 \geq \frac{4A_M \cdot B_M(K_1 + A_M)}{B_m^2 \cdot B_m(K_1 - A_M)} \quad (18)$$

where $A_M \geq |A|$ and $B_M \geq B \geq B_m$ are the superior and inferior bounds of A and B , respectively, in the second derivative of y .

$$\frac{d^2 y}{dt^2} = A(x,t) + B(x,t) \frac{du}{dt} \quad (19)$$

4 SIMULATION RESULTS

Simulations are carried out with a 1.5 MW DFIG operating in to a 398 V/50 Hz grid by using the Matlab/Simulink environment. Parameters of the machine are given in Table. Both control strategies, C-DPC and SOCSM-DPC, are simulated and compared in terms of reference tracking, stator-current harmonic distortions and robustness against the machine-parameter variations.

4.1. Reference tracking test

The aim of this test is to verify the performance of the proposed strategy when the DFIG speed is considered constant at its nominal value. The simulated results are

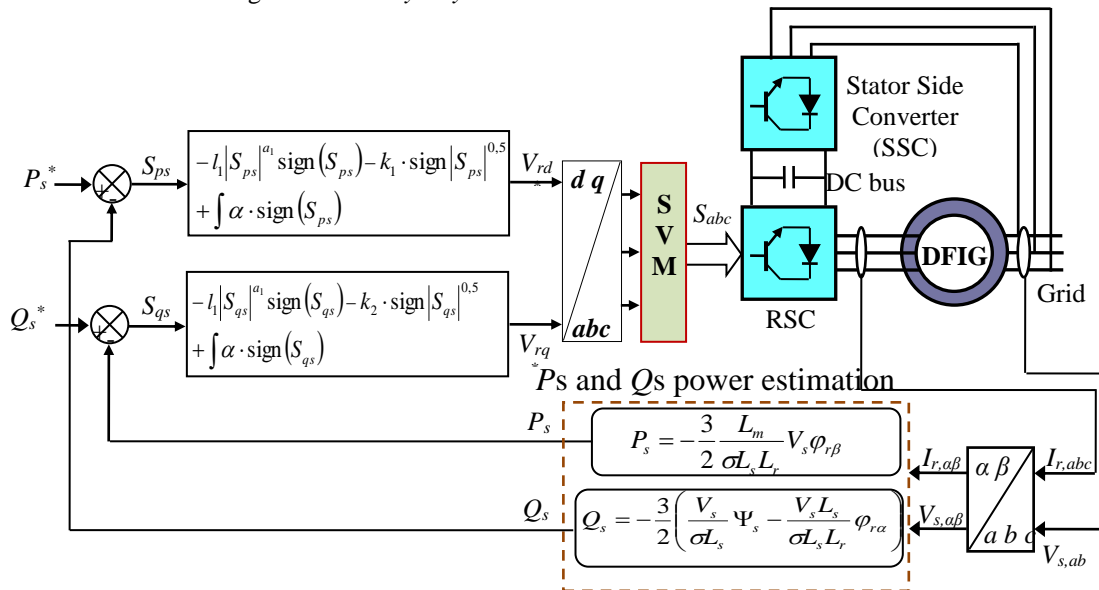


Figure 3. Schematic diagram of DFIG-based SOCSM-DPC.

shown in figures 4 to 6. As presented by Figures 4 and 5, both controllers track correctly their reference steps and there is no static error. Furthermore, SOCSM-DPC ensures decoupling between the two axes contrary to C-DPC. Further tests are shown in Figure 6 demonstrating the total harmonic distortions (THD) of the stator current of the generator by using the Fast Fourier Transform (FFT) method for both DPC control schemes. As clearly seen, the SOCSM-DPC control reduces THD down to 58.45% compared to C-DPC where THD is 77.71% by alleviating the chattering phenomenon.

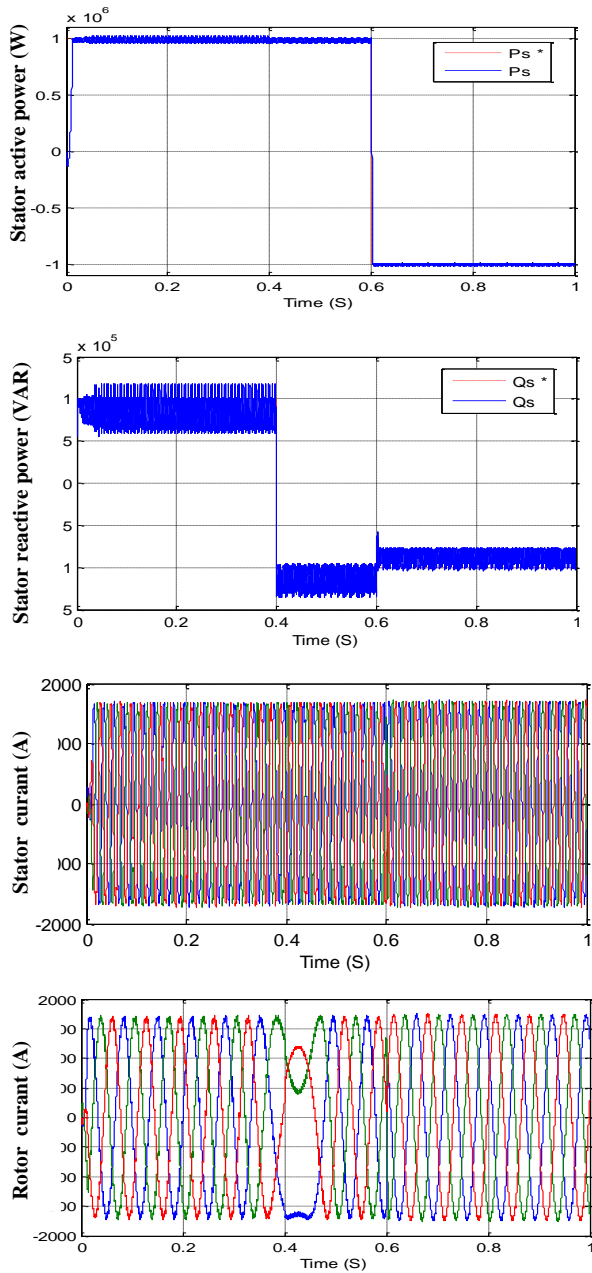


Figure 4. C-DPC strategy responses (reference tracking test).

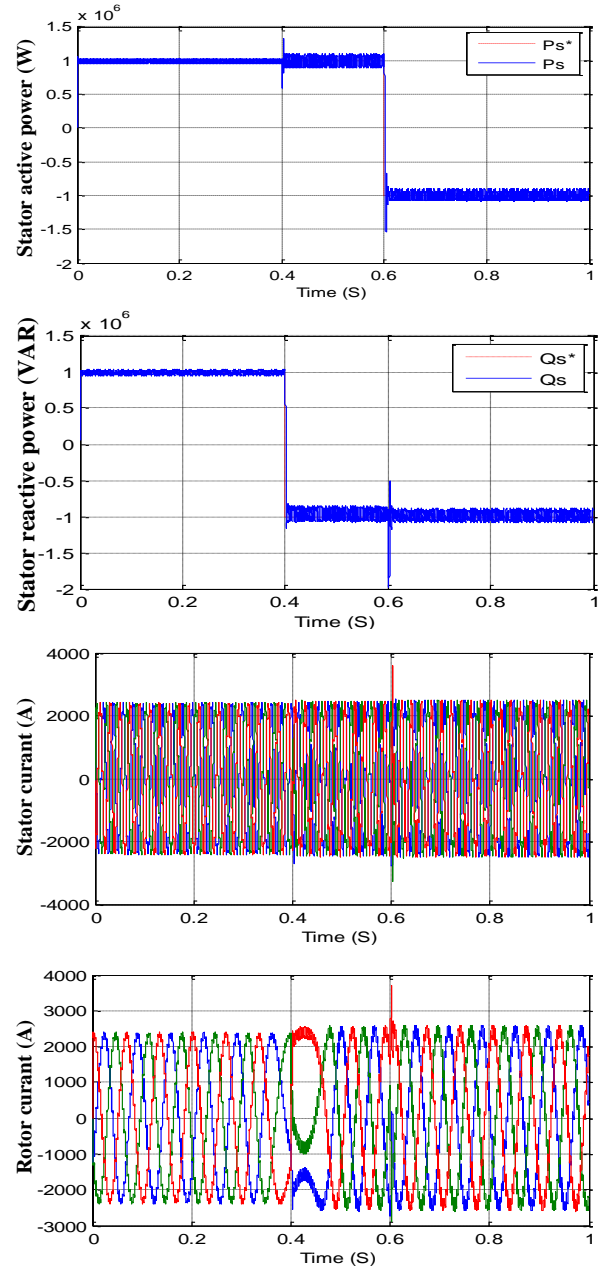


Figure 5. SOCSM-DPC strategy responses (reference tracking test).

4.2. Robustness test

The robustness of the proposed DPC-based SOSM control algorithm for a machine running at its nominal speed is analyzed for the variable machine parameters. Variations in the values of the stator and rotor resistances and in the values of inductances are taken into account for checking the robustness of the control scheme in the simulation. For this reason, the values of resistances R_s and R_r are doubled and the values of inductances L_s , L_r and M are divided by 2. Simulation results are shown in figures 7 to 9. As seen from these figures, there are hardly any differences between such high parameter variation values of DFIG for the

proposed SOSM-DPC scheme, contrary to the C-DPC strategy where the time response increases slightly. Therefore, robustness of the novel SOSM-DPC scheme to the DFIG parameter variations is also confirmed.

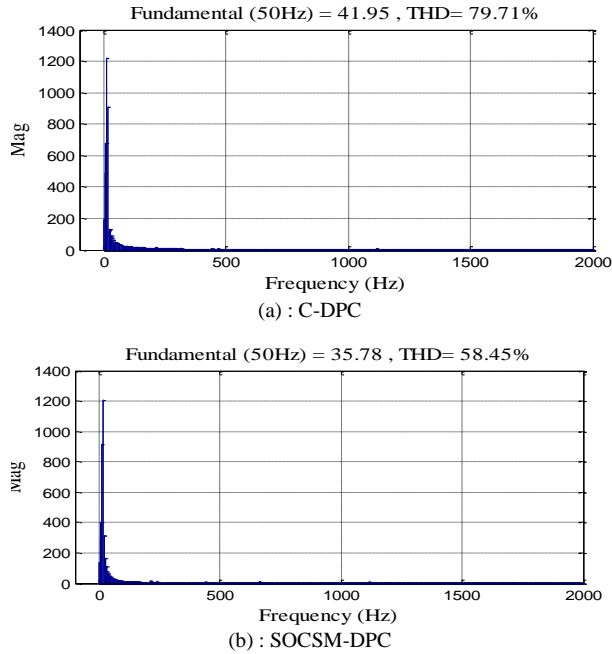


Figure 6. Spectrum harmonic of a one-phase rotor current.

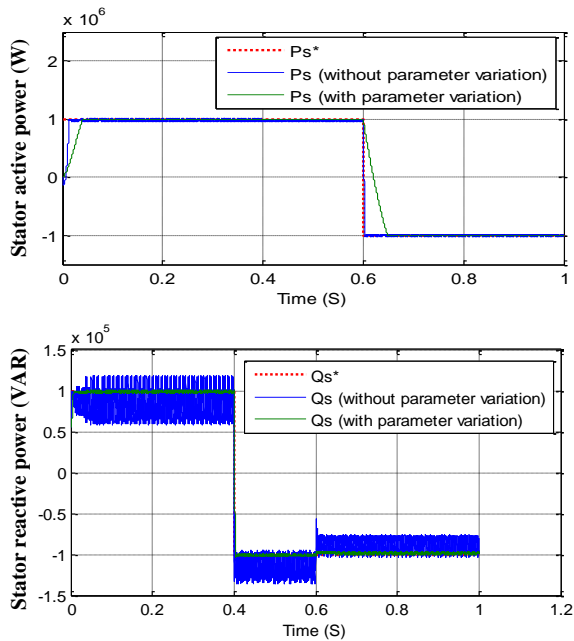


Figure 7. C-DPC strategy responses (robustness test).

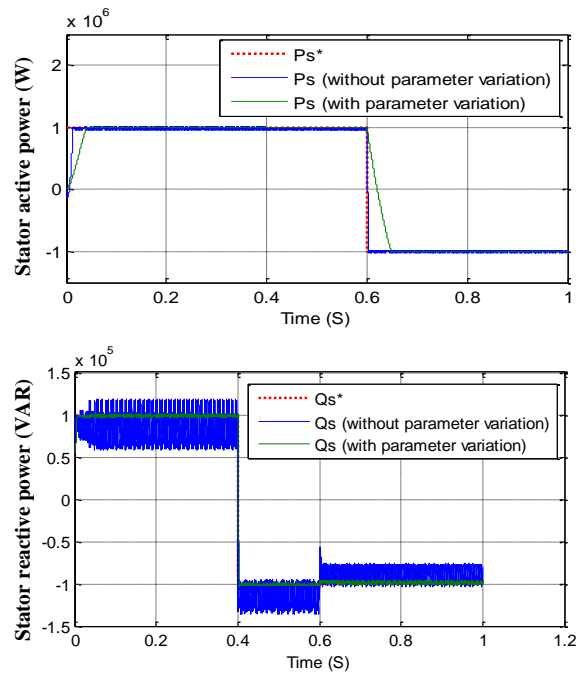


Figure 8. SOCSM-DPC strategy responses (robustness test)

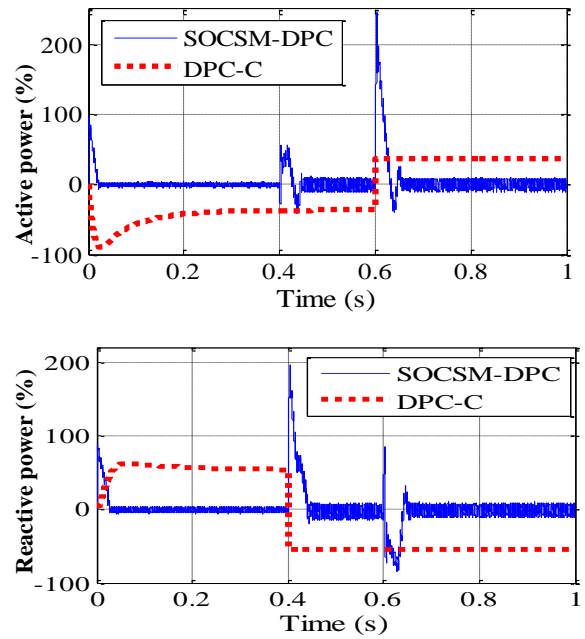


Figure 9. Error curves (robustness test).

5 CONCLUSION

The paper proposes an SOCSM DPC scheme for a grid-connected DFIG system. The scheme is implemented on a 1.5 MW wind-turbine DFIG system. Simulation results show an enhanced transient response and reduced chattering in the controlled quantity by using the proposed controller as compared to C-DPC. The results also prove robustness parameter variations of the machine. SOCSM-DPC based on the obtained results, it can be concluded that the robust control method can be a very attractive solution for devices using DFIG, such as wind-energy conversion systems.

Table 1. The DFIG parameters.

Parameters	Rated Value	Unity
Nominal power	1.5	MW
Stator frequency	50	Hz
Number of pairs	2	/
Stator resistance	0.012	Ω
Rotor resistance	0.021	Ω
Stator inductance	0.0136	H
Rotor inductance	0.0136	H
Mutual inductance	0.0135	H
Inertia	1000	Kg.m^2
Viscous friction	0.0024	Nm/sV

6 REFERENCES

- [1] M. Edrah, K.L. Lo, O. Anaya-Lara: Impacts of high penetration of DFIG wind turbines on rotor angle stability of power systems, In: IEEE T Sustain Energ, vol. 6, No. 3, pp. 759-766, 2015.
- [2] R.Bouzidi, A. Allag, A. Chouder: Improved DTC algorithm for reducing torque and flux ripples of induction motor, In: Mediterranean Journal of Measurement and Control Vol.12, No.2, pp. 561-570, April 2016.
- [3] P. Cartwright, L. Xu: Direct active and reactive power control of DFIG for wind energy generation, In: IEEE Trans. Energy Convers, vol.21, No. 3, pp. 750 – 758, 2006.
- [4] A. Madhukar Rao, N. Kiran Kumar, K. Sivakumar: A multi-level inverter configuration for 4n pole induction motor drive by using conventional two-level inverters, In: IEEE International Conference on Industry Technology, pp. 592-597, 17-19 March 2015.
- [5] K. D. Kerrouche, A. Mezouar, L. Boumediene, A. V. D. Bossche: Speed sensorless and robust power control of grid connected wind turbine driven doubly fed induction generators based on flux orientation, In: Mediterranean Journal of Measurement and Control Vol. Vol. 12 No. 3, pp. 606-618, 2016
- [6] X. Zhu, S. Liu, Y. Wang: Second-order sliding-mode control of DFIG-based wind turbines, In: IEEE 2014 3rd Renewable Power Generation Conference, pp. 1-6, 24-25 September 2014.
- [7] F. Amrane, A. Chaiba: Hybrid Intelligent Control based on DPC for grid connected DFIG with a Fixed Switching Frequency using MPPT Strategy, In: IEEE 4th international conference on electrical engineering, pp. 1-4, 2015.
- [8] A. Daoud, F. Ben Salem: Direct Power Control of a Doubly Fed Induction Generator Dedicated to Wind Energy Conversions, In: IEEE 11th international multi-conference on systems, signals and devices, pp.1-8, 2014.
- [9] O. Chandrasekhar, K. Chandra sekhar: Five-level SVM Inverter for an Induction motor with Direct Torque Controller, In: Journal of Electrical Engineering, vol.13, No.4, pp.53-61, 2013.
- [10] B. Beltran, M. H. benbouzid, T. Ahmed-Ali: High-order sliding mode control of a DFIG-based wind turbine for power maximization and grid fault tolerance, In: IEEE Electric Machines and Drives Conference IEMDC'09, vol. 1, pp.183-189, 2009.
- [11] Beltran, M. H. benbouzid, T. Ahmed-Ali: Second-Order Sliding Mode Control of a Doubly Fed Induction Generator Driven Wind Turbine, In: IEEE transactions on energy conversion, vol. 27, No. 2, June 2012.
- [12] A. Hamache, O. Bensidhoum, H. Chekireb: Multivariable second order sliding mode based controller for unified power flow controller, In: Mediterranean Journal of Measurement and Control Vol. 11, No.4, pp. 483 - 491 October 2015.
- [13] C. Wei, W. Qiao, Y. Zhao: Sliding-Mode Observer-Based Sensorless Direct Power Control of DFIGs for Wind Power Applications, In: IEEE power and energy society general meeting (PES), pp. 1-5, 2015.
- [14] P. Ankit, A. Shah, J. Mehta: Direct Power Control of DFIG Using Super-Twisting Algorithm Based on Second-Order Sliding Mode Control, In: IEEE 14th international workshop on variable structure systems (VSS), pp.136-141, 2016.
- [15] S. Li, T. Haskew: Energy Capture, Conversion, and Control Study of DFIG Wind Turbine under Weibull Wind Distribution, In: IEEE power and energy society general meeting (PES), pp 1-9, 2009.
- [16] S. Kahla, Y. Soufi, M. Sedraoui, M. Bechouat: On-Off control based particle swarm optimization for maximum power point tracking of wind turbine equipped by DFIG connected to the grid with energy storage, In: Int J Hydrogen Energ, vol.40, pp.13749-13758, 2015.
- [17] A. Bakouri, A. Abbou, H. Mahmoudi, K. Elyalaoui: Direct torque control of a doubly fed induction generator of wind turbine for maximum power extraction, In: IEEE International Renewable and Sustainable Energy Conference, pp. 334-339, 17-19 October 2014, Morocco.
- [18] G. S. Buja, M. P. Kazmierkowski: Direct torque control of PWM inverter-fed AC motors - a survey, In: IEEE transactions on industrial electronics, vol. 51 No. 4, pp.744-757, 2004.
- [19] Y. Djeriri, A. Meroufel, A. Massoum, Z. Boudjema: A comparative study between field oriented control strategy and direct power control strategy for DFIG, In: Journal of Electrical Engineering, Vol. 14, No. 2, pp. 159-167, 2014.
- [20] F. Cupertino, D. Naso, E. Mininno, B. Turchiano: Sliding-mode control with double boundary layer for robust compensation of payload mass and friction in linear motors, In: IEEE Trans. On Industry Applications, Vol. 45, No. 5, pp. 1688-1696, Sep./Oct 2009.
- [21] A. Levant: Quasi-continuous high-order sliding-mode controllers, In: IEEE transactions on automatic control, vol. 50, No. 11, pp.1812-1816, 2005.
- [22] C. Edwards, Y. Shtessel: Adaptive Continuous Higher Order Sliding Mode Control, In: Preprints of the 19th World Congress, the International Federation of Automatic Control, pp. 10826-10831, August 24-29 2014, Cape Town, South Africa.

Abdelkader Bouyekni He received his M.Sc degree, in Electrical Engineering in 2010 from the University of Sciences and technology of Oran, Algeria. He is currently working towards his Ph.D degree in the LGEER Laboratory (Laboratoire Génie Electrique et Energies Renouvelables). His research interest includes intelligent control strategies, electrical machine drives, renewable energies, optimization and systems modeling and control. Email: aek.bouyekni81@gmail.com

Rachid Taleb received the M.SC. degree in electrical engineering in 2004 from the Hassiba Benbouali University, Chlef, Algeria, and his the Ph.D. degree in electrical engineering in 2011 from the Djillali Liabes University, Sidi Bel-Abbes, Algeria. He is currently an Associate Professor at the Department of Electrical Engineering, Hassiba Benbouali University. He is a team leader in the LGEER Laboratory (Laboratoire Génie Electrique et Energies Renouvelables). His research interest includes intelligent control, heuristic optimization, control theory of converters and converters for renewable energy sources. Email: rac.taleb@gmail.com.

Zinelaabidine Boudjema received his M.SC. degree in Electrical Engineering in 2010 from ENPO, Oran, Algeria, and his Ph.D. degree in Electrical Engineering in 2015 from Djillali Liabes University, Sidi Bel abbes, Algeria. He is currently an Associate Professor at Electrical Engineering Department at the Hassiba Benbouali University. His research interests include power electronics, electrical machine robust control and renewable energies. Email: z.boudjema@univ-chlef.dz

Housseyn Kahal received M.SC degree, in Electrical Engineering in 2013 from the University of Sciences and technology of Oran, Algeria. He is currently working towards his Ph.D. degree at the LGEER Laboratory (Laboratoire Génie Electrique et Energies Renouvelables). His research interest includes intelligent control strategies, electrical machine drives, renewable energies, optimization and systems modeling and control. Email: hous.kahal@gmail.com